Available online at www.sciencedirect.com
ScienceDirect
Control Engineering Practice 15 (2007) 421–433
CONTROL ENGINEERING PRACTICE
www.elsevier.com/locate/conengprac

Grey-box identification of air-handling unit elements

Christian Ghiaus*, Adriana Chicinas, Christian Inard

Laboratoire d'étude des phénomènes de transfert appliqués au bâtiment (LEPTAB), Université de La Rochelle, Av. M. Crépeau, 17000 La Rochelle, France

Received 25 October 2005; accepted 15 August 2006
Available online 10 October 2006

Abstract

The air-handling units (AHUs) provide complete control of temperature and humidity in air-conditioned spaces. The models of the AHU elements are nonlinear and the controlled variables, temperature and relative humidity, coupled. This paper demonstrates that in the case of sensible heat exchange without moisture removal if the outputs of the electric coils, fluid-filled coils and steam humidifiers of an AHU are considered to be the differences between the air temperature and the humidity ratio of the outlet and the inlet, then the models may be written as the product of a static and a dynamic gain. The parameters of the discrete form of these models are experimentally identified. The dynamics of the elements and of their sensors are very similar. Therefore, the parameter identification of the elements takes into account the model of the sensor, previously identified. This grey-box approach combines theoretical modelling, parameter identification of discrete models and parameter identification of partially known models by using optimization techniques.

Keywords: Building automation; Energy management systems; Heat exchangers; Decoupled subsystems; Autoregressive models; Transfer functions

1. Introduction

In air-conditioned buildings equipped with forced-air distribution systems, the air-handling units (AHU) are used to control one or more of the following parameters of the supply air: temperature, θ_{sa}, relative humidity, ϕ_{sa}, and air velocity. These systems may be of constant or variable air volume. The constant air volume systems have fixed-speed fans and control the temperature and the humidity of the building by varying the temperature and the humidity of the supplied air. With a variable air volume system, the airflow is controlled. Hereafter, the case of AHU in constant air volume systems is considered.

AHUs may have different configurations. Fig. 1 presents a typical constant air AHU composed of a preheating coil, HC_1, a cooling coil, CC, a reheating coil, HC_2, and a steam humidifier, H. Three dampers, which are actuated simultaneously, combine the air from outside and the air recirculated from the building to form the mixed air which is then conditioned by the AHU and supplied to the building through the air distribution system. The air-conditioning processes that occur typically in an AHU are shown in Fig. 2: heating and humidification (processes 2–3–4), dry-cooling and humidification (processes 1–3–4), and simultaneous sensible cooling and dehumidifiation and then heating (processes I–II–4). The temperature and the humidity of the mixed air (states 1, 2 and I in Fig. 2) and of the supply air (state 4 in Fig. 2) vary due to fluctuating weather conditions and building occupancy.

The control problem of an AHU is how to command its elements (cooling coil, heating coils and humidifier) in order to control the temperature, θ_{sa}, and the relative humidity, ϕ_{sa}, of the supply air. A first complication comes from the fact that the controlled variables are coupled: a change in the air temperature, θ, generates a change in the relative humidity, ϕ, and vice versa (Fig. 2). A second difficulty is due to the variable load. For the same command value, u, of an AHU element, the temperature and relative humidity (θ_{a2}, ϕ_{a2}) of the outlet air will be different depending on the temperature and relative humidity (θ_{a1}, ϕ_{a1}) of the inlet air. A third hindrance is the inherent nonlinearity of the AHU elements. Further problems are due to the time varying characteristics of the elements, valve hysteresis and stiction,

*Corresponding author. Tel.: +33 5 4645 7259; fax: +33 5 4645 8241.
E-mail address: cghiaus@univ-lr.fr (C. Ghiaus).

0967-0661/$ - see front matter
doi:10.1016/j.conengprac.2006.08.005

Nomenclature

$\mathbf{A}_D$	matrix of observations
c	specific heat (kJ/kg K)
$\mathbf{e}$	vector of errors (modelling and random noise)
G	transfer function
h	enthalpy (kJ/kg)
m	mass (kg)
P	power (W)
Q	volumetric flow (m^3/s)
S	surface (m^2)
T	time constant (s)
T_s	sampling time (s)
U	overall heat transfer coefficient (W/(m^2K))
u	input variable for the process
$\mathbf{u}$	vector of input values
v	velocity (m/s)
W	humidity ratio of moisture per dry air (g/kg)
$\mathbf{x}$	vector of states
y	output variable
$\mathbf{y}$	vector of output values

Symbols for domain variables

t	time domain (s)
s	Laplace variable in s domain, $s = \sigma + j\omega$ (s^{-1})
z	variable in z domain, $z = e^{sT_s}$
q^{-1}	backward shift operator in sampled-time domain $q^{-1}u(t) = u(t - T_s)$

Greek letters

ϕ	relative humidity (%)
θ	temperature (K)
τ	transport time (s)
$\boldsymbol{\psi}$	vector of parameters
$\hat{\boldsymbol{\psi}}$	vector of estimated parameters

Subscripts

1	inlet
2	outlet
a	air
C	coil (heating or cooling)
d	dry
M	maximum
m	mixed
s	sampling
T	transducer (sensor)
w	water

Superscript

T	transpose of matrix

etc. This paper focuses on finding models that alleviate the first three problems.

The non-stationary plant operation associated with the nonlinearity of the AHU elements and the coupling of the controlled variables makes the AHU control a non-trivial problem (Ghiaus, 1996; Underwood, 1999). The development of building automation technology offers the opportunity to implement sophisticated control algorithms to respond to this problem. Variable weather conditions and building occupation modify very quickly the operating point of the AHU causing a fast change in the static gain of the loop. The PID control loop becomes either too sluggish or too responsive (and often oscillatory). The poor quality of AHU controls is one of the causes for occupants dissatisfaction (Levermore, 2000) and has been accepted in practice only because of the lack of catastrophic consequences (Underwood, 1999). It should be mentioned that heating and air conditioning consume about one third of the primary energy and that the indoor comfort influences the productivity, especially in office buildings. It is estimated that the avoidable energy waste in buildings is in the range of 20–50% and that 15% of the energy waste can be avoided by a good control of the systems (Levermore, 2000).

Since classical PID solutions cannot solve the AHU control problem, some approaches consider the whole AHU as a multiple-input multiple-output (MIMO) black box and use a variant of adaptive tuning in techniques of adaptive, fuzzy, neural network or genetic algorithms control (Bi et al., 2000; Ghiaus, 1996, 2001; Salsbury, 2002, 2006; Singh, Zaheer-uddin, & Patel, 2000; So, Chan, Chow, & Tse, 1995; Sousa, Babuska, & Verbruggen, 1997; Thompson & Dexter, 2005; Tobi & Hanafusa, 1991; Wang & Jin, 2000; Wang & Xu, 2002).

The problem with adaptive tuning is that time is needed to gather data in order to find the new parameters of the controller. These techniques are suited when the values of the parameters are varying slowly. An alternative to adaptive tuning is gain scheduling. The nonlinear characteristic of the AHU may be obtained from measurements or from models and then the parameters of the controller can be adjusted according to the operation point (Deng, 2002; Ghiaus, 1996, 2001; Thompson & Dexter, 2005). In other approaches, multivariable compensators are designed taking into account the physical laws of the humid air (Underwood, 1999). The decoupling of the controlled variables may be obtained by using the orthogonality of the temperature, θ, and the humidity ratio, W (Fig. 2). The humidity ratio, W, is calculated from the values of the temperature, θ, and the relative humidity, ϕ, for the set point and for the output. The control is then done for temperature and humidity ratio (Howell, 1988).

Explicitly or implicitly, all these algorithms are synthesized by using the model of the AHU as a controlled system. The model can be a white box, a black box or a

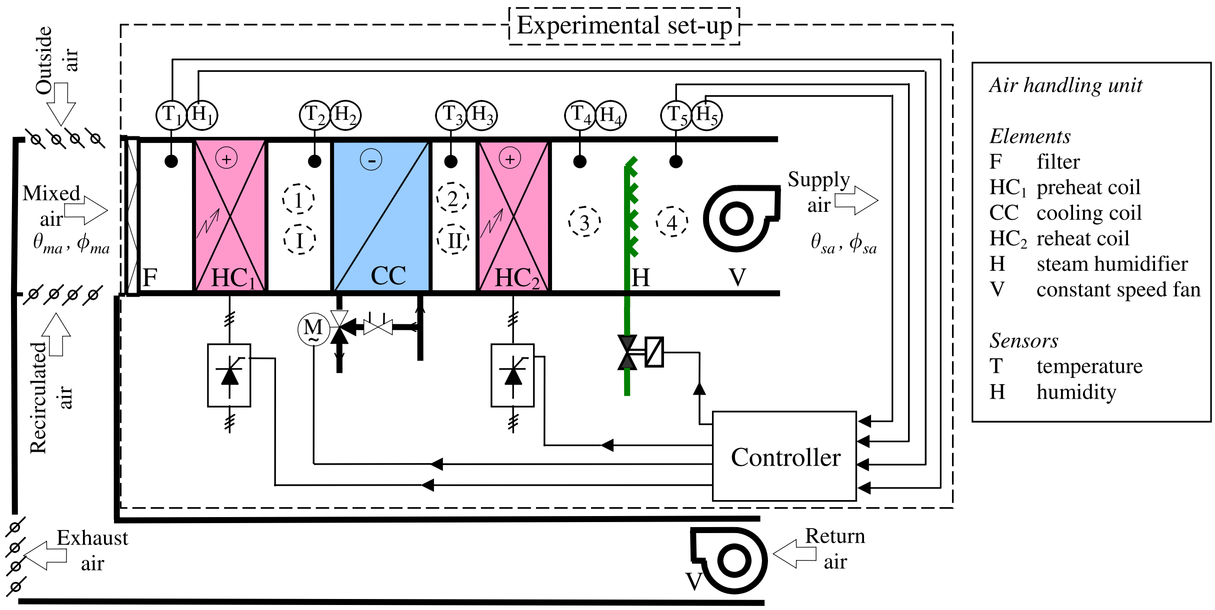

Fig. 1. Air-handling unit (AHU).

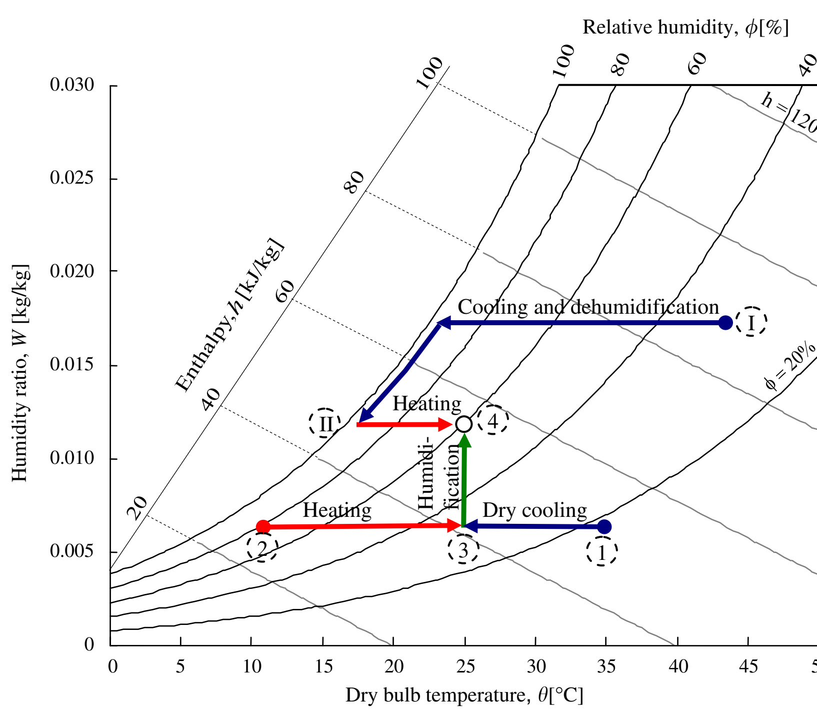

Fig. 2. Processes in the air-handling unit represented in the psychrometric chart.

grey box. The white-box models, which are based on theoretical considerations, are included in software for building performance simulation. This software is used to emulate the AHU in model-based control (Clarke et al., 2002; Mathews & Botha, 2003) or in control loop diagnosis (Salsbury, 1999; Wang & Zheng, 2001). The black-box models, which represent input–output relations that fit the measurements, are used in practical applications of control. They are obtained by experimental identification techniques such as Ziegler–Nichols, parameter identification (Pakanen & Sundquist, 2003), relay plus step tests (Bi et al., 2000), etc. If the models obtained are linear, they are valid around a static operating point (Kramer, 2003; Shin, Chang, & Kim, 2002; Tashtoush, Molhim, & Al-Rousan, 2005). In grey-box modelling, the structure of the model is obtained from first principles and the parameters of the models are obtained from measurements. This approach is especially useful for control applications when the model is expressed in a suitable form such as transfer function or state space.

Many grey-box models of the coils consider the processes of heating, dry cooling and humidification (transformations 2–3–4 and 1–3–4 in Fig. 2). This is justified by the fact that the set point of the indoor temperature is typically a fixed value within the comfort zone during the occupied time and that the zone humidity is allowed to "float" within a range dictated by the system design (ASHRAE, 1999). Some regulations even forbid dehumidification by cooling (COSTIC, 2003). Grey model transfer functions with distributed parameters for the water–air finned coils were obtained from the geometrical specifications of the coil and the physical properties of the air, water and metal (Gartner & Daane, 1969; Gartner & Harrison, 1963, 1965). In a further development, a first-order model of the coil was obtained (Gartner, 1972; Pearson, Leonard, & McCutchan, 1974). In other approaches, Kalman filtering is used for identification of the parameters of a state-space representation of the model obtained from physical considerations (Jonsson & Palsson, 1994).

A further complication occurs when the air is dehumidified (transformations I–II–4 in Fig. 2); the coil may be partially or totally wet presenting a variable heat transfer coefficient. A control model for wet coils may be obtained by estimating the cooling load from measurements on the water side (Jin, Cai, Wang, & Yao, 2005; Wang et al., 2004).

In general, the models of the AHU, either theoretical or experimental, do not consider separately the AHU element and its sensor, although it turns out that in practical applications the dynamics of the elements and of the sensors are comparable. If known, the dynamic model of the sensor may be easily integrated when the theoretical approach is used. However, in the black-box approach, the models used for parameter identification consider the sensor and the element as a single process. Consequently, the dynamic gain due to the sensor is not revealed, although it is very important.

The aim of this work is to find a simple way to improve the control of constant air-volume AHU by formulating the models of its elements so that they become single-input single-output and linear on the whole range of operation. Modelling the processes in this way results in a control strategy that may be considered similar to gain scheduling with the difference that the PID control algorithm is with fixed parameters on the whole range of operation.

This paper deals only with the modelling and parameter identification of the elements of an AHU designed to supply constant air volume without dehumidification: fluid-filled cooling coil, electric heating coils and direct steam injection humidifier (Fig. 1). The processes considered are heating with humidification and cooling with humidification (Fig. 2). The AHU is a MIMO system with three inputs, the commands of the cooling coil, heating coil and humidifier, and two outputs, the supply air temperature and humidity ratio (Fig. 1). Note that the preheating coil is used to protect the cooling coil from freezing; its command is related to the reheating coil. The sensors are identified separately by using a step response. This information is then used to identify the model parameters of the element. For each element, the model structure is obtained by discretization of the continuous model derived from physical principles. The model parameters are identified by using a grey-box approach in which the parameters of the sensor are known.

This paper takes advantage of the fact that the airflow rate is constant and that there is no condensation on the cooling coil and considers the variation of the dry-bulb temperature, θ, and of the humidity ratio, W, as being the outputs of each element. It is demonstrated that, consequently, each element changes only one variable: the coils change the temperature difference and the humidifier changes the humidity ratio difference.

2. Experimental set-up

The experiments were conducted on a commercial AHU equipped with a commercial controller, represented inside the dashed rectangle in Fig. 1. The AHU, 0.80 m high by 0.50 m wide, is composed of a filter, a finned water-filled cooling coil, two electric heating coils, a steam humidifier and a constant speed fan. The constant airflow in the AHU is $Q_a = 0.33\,\mathrm{m^3/s} \cong 1200\,\mathrm{m^3/h}$; it was measured by using the tracer gas method. The mean air velocity in the AHU is $v_a = 0.82\,\mathrm{m/s}$; it was measured in a section on a grid of 4×4 equally spaced points by using hot-wire anemometers. The airflow rate and the mean speed are in perfect accordance. The water-filled finned coil which cools the air (process 1–3 in Fig. 2) is controlled by a three-way valve with a linear characteristic (Figs. 3 and 4). The time constant of the valve positioner is about 15 s. The balance valve on the by-pass was set to have the same pressure drop as the cooling coil. The coil is connected to a chiller which delivers water with the temperature varying between 7 and 10 °C. When the temperature of the supplied water, θ_S, is higher than 10 °C, the chiller is turned on until the temperature of the supply water, θ_S, falls below 7 °C. In dry cooling, the mean air temperature drop over the

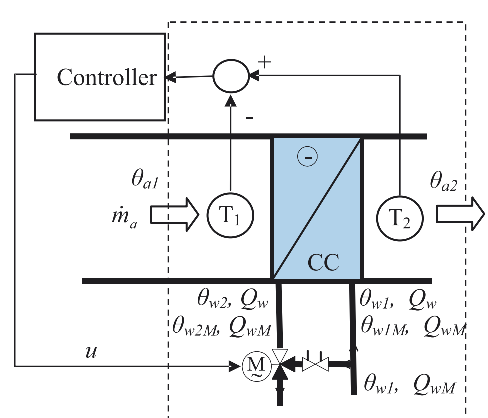

Fig. 3. Fluid-filled cooling coil.

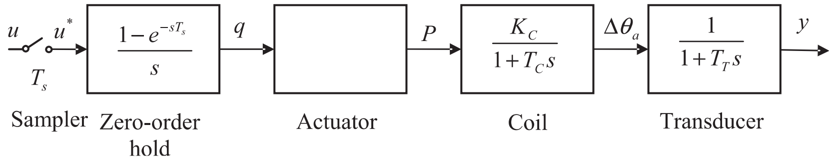

Fig. 4. Block diagram of the open-loop sampled data system represented by the coils. The model of the actuator is given by Eq. (27) for the electrical coil, and by Eqs. (44) and (45) for the cooling coil.

Table 1
Measured air transformations in the AHU elements (see Fig. 5)

Command	Electrical coils		Cooling coil CC	Steam humidifier
	HC_1	HC_2		H
u (%)	$\Delta\theta$ (°C)	$\Delta\theta$ (°C)	$\Delta\theta$ (°C)	ΔW (g/kg)
0.00	0.0	0.0	0.0	0.00
0.25	3.4	6.4	−10.1	0.37
0.50	6.9	12.6	−12.0	1.53
0.75	9.3	18.4	−13.9	3.00
1.00	11.3	24.0	−14.5	3.99

cooling coil for the maximal water flow rate is 14.5 °C (Table 1 and Fig. 5a). This corresponds to a maximal power of the cooling coil of 5.74 kW.

Two electric coils with maximal power of 4.3 and of 9.5 kW, respectively, were tested. At maximum power, the two electric coils increased the air temperature with 11.3 and 24.0 °C, respectively (Table 1 and Fig. 5a). The power delivered by the electric coils was varied by using a time-proportional command of a static relay for a given percentage of time during 1 min.

The humidifier injects steam into the air stream increasing the air humidity (process 3–4 in Fig. 2). The maximum steam flow mass is $\dot{m}_{wM} = 6$ kg/h, which, for the dry air mass flow $\dot{m}_{da} = 1500$ kg/h, generates an increase of 4 g of water per kg of dry air, $\Delta W = 4\,g/kg$ (Table 1 and Fig. 5b).

The processes studied were heating and humidification (states 2–3–4 in Fig. 2) and dry cooling and humidification (states 1–3–4 in Fig. 2). The temperature and humidity sensors T_1H_1, T_2H_2, T_3H_3, T_4H_4 and T_5H_5 were used for experimental measurements (Fig. 1). In real situation, only the sensors T_1H_1 and T_5H_5 are needed.

3. Parameter identification of transducer model

Assuming that the temperature of the sensor is homogenous, the energy balance for the transducer may be expressed by

$$m_T c_T \frac{\mathrm{d}\theta_T}{\mathrm{d}t} = U_T S_T(\theta_a - \theta_T), \tag{1}$$

where the left-hand term represents the variation of heat accumulation in the metal mass of the sensor and the right-hand term is the rate of heat transfer by convection from the air to the sensor.

Considering the air temperature, θ_a, as the input and the temperature of the metal mass of the sensor, θ_T, as the output, the transfer function corresponding to the differential equation (1) is

$$G_T(s) \equiv \frac{\theta_T(s)}{\theta_a(s)} = \frac{K_T}{1 + T_T s}, \tag{2}$$

with the static gain $K_T = 1$ and the time constant $T_T = R_T C_T$, where R_T is the thermal resistance of the transducer, $R_T = 1/(U_T S_T)$, and C_T is its thermal mass, $C_T = m_T c_T$. A first-order model

$$G_H(s) \equiv \frac{\phi_H(s)}{\phi_a(s)} = \frac{K_H}{1 + T_H s} \tag{3}$$

was chosen also for the humidity sensor. In order to use the time series resulting from the sampled data, the transfer function (2) should be transformed in z domain by using the relation $z = e^{sT_s}$. An approximation of this relation is the bilinear transform

$$s \cong \frac{2}{T_s}\frac{1 - z^{-1}}{1 + z^{-1}}. \tag{4}$$

The discrete form of model (2) is obtained by applying the bilinear transform (4):

$$G_T(z^{-1}) = \frac{b_0 + b_1 z^{-1}}{1 + a_1 z^{-1}}, \tag{5}$$

where

$$b_0 = b_1 = \frac{K_T T_s}{2T_T + T_s} \tag{6}$$

and

$$a_1 = \frac{T_s - 2T_T}{2T_T + T_s}. \tag{7}$$

Noting the output with y and the input with u, Eq. (5) gives an input–output discrete model

$$y(t) + a_1 y(t - T_s) = b_0 u(t) + b_1 u(t - T_s) \tag{8}$$

or written by using the backward shift operator, q^{-1},

$$\frac{y(t)}{u(t)} = \frac{B(q^{-1})}{A(q^{-1})}, \tag{9}$$

where $A(q^{-1}) = 1 + a_1 q^{-1}$ and $B(q^{-1}) = b_0 + b_1 q^{-1}$.

By noting:

$$\mathbf{y} \equiv [\,y(t) \quad y(t-1) \quad \cdots \quad y(t-m)\,]^{\mathrm{T}}, \tag{10}$$

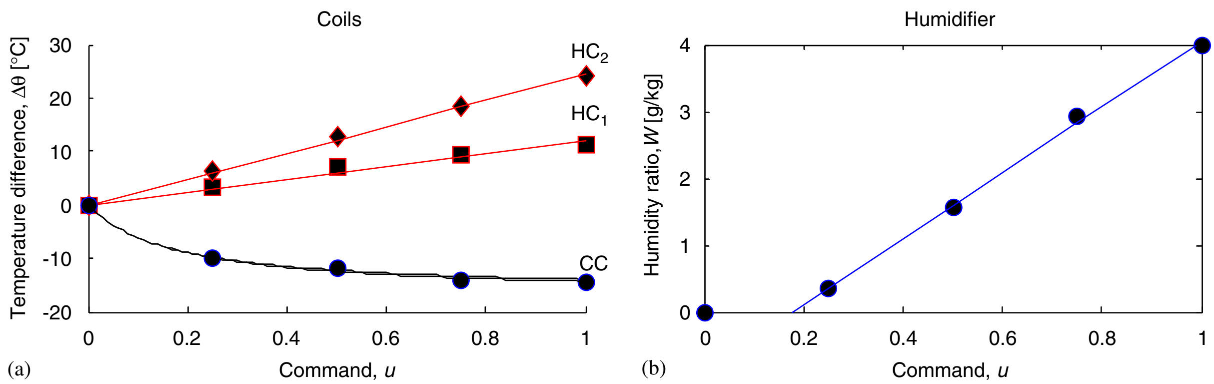

Fig. 5. Static characteristics: (a) heating coil 1 (HC_1), heating coil 2 (HC_2) and cooling coil (CC); (b) humidifier.

Table 2
Typical identified values for a temperature and humidity sensor (sampling time $T_s = 1/6$ (min))

Sensor	Discrete model	Continuous model	
		Static gain K	Time constant T (min)
Temperature	$A(q^{-1}) = 1–0.8564\,q^{-1}$ $B(q^{-1}) = 0.07432 + 0.07432\,q^{-1}$	1.035	1.08
Humidity	$A(q^{-1}) = 1–0.9190\,q^{-1}$ $B(q^{-1}) = 0.04299 + 0.04299\,q^{-1}$	1.062	1.97

$$\mathbf{A}_D \equiv \begin{bmatrix} y(t-1) & u(t) & u(t-1) \\ y(t-2) & u(t-1) & u(t-2) \\ \vdots & \vdots & \vdots \\ y(t-m-1) & u(t-m) & u(t-m-1) \end{bmatrix} \tag{11}$$

and

$$\boldsymbol{\psi} \equiv [a_1 \quad b_0 \quad b_1]^{\mathrm{T}}, \tag{12}$$

model (8) can be written in matrix form as

$$\mathbf{y} = \mathbf{A}_D\boldsymbol{\psi} + \mathbf{e}, \tag{13}$$

where an error vector, $\mathbf{e}$, was incorporated to account for random noise and modelling error.

The estimation of the parameters, $\hat{\boldsymbol{\psi}}$, minimizes the sum of squared errors:

$$E(\boldsymbol{\psi}) = \mathbf{e}^{\mathrm{T}}\mathbf{e}, \tag{14}$$

where $\mathbf{e} = \mathbf{y} - \mathbf{A}_D\boldsymbol{\psi}$ is the error vector produced by a specific choice of $\boldsymbol{\psi}$. If the matrix $\mathbf{A}_D^{\mathrm{T}}\mathbf{A}_D$ is non-singular, then $\hat{\boldsymbol{\psi}}$ is unique and given by

$$\hat{\boldsymbol{\psi}} = (\mathbf{A}_D^{\mathrm{T}}\mathbf{A})^{-1} \times \mathbf{A}_D^{\mathrm{T}}\mathbf{y}. \tag{15}$$

Having the estimated parameters $\hat{\boldsymbol{\psi}}$ from Eq. (15), the parameters T_T and K_T of the continuous model may be obtained from Eqs. (6) and (7). Note that two values of K_T may be obtained from Eq. (6). The static gain may be also estimated from:

$$K_T = \frac{\sum_{j=0}^{m} b_j}{1 + \sum_{i=1}^{n} a_i}. \tag{16}$$

A large difference between these three values indicates a poor estimation of the parameters.

Parameter identification requires the excitation of all the modes of the system. A simple signal that contains a large frequency spectrum is the step input. It may be easily obtained by extracting the temperature and humidity sensors from the AHU, waiting that their indication stabilizes, introducing back the sensors in the AHU and waiting that the signal stabilizes. The identification of the sensor may be done in factory, by the manufacturer of the AHU, or in situ, by the commissioning engineer. Note that in practice only the sensors T_1H_1 and T_5H_5 are needed because the processes of heating/cooling and humidification are decoupled (see Sections 4 and 5).

Table 2 shows typical values for a temperature and humidity sensor identified by using Eq. (15). Note that the static gain is very near to one, showing a good calibration and that the time constants for temperature and humidity are different.

4. Parameter identification of coil models

The coil model introduced in this paper considers as output the temperature difference between the outlet and the inlet air and as input the power delivered by the coil. For the cooling coil, the power delivered by the coil is controlled by a three-way valve. The time constant of the valve positioner is 15 s; it is negligible in comparison with the time constants of the cooling coil and of the temperature sensor. For the heating coil, the power is varied by a static relay in accordance with the command received from the controller. The command is time-proportional with a cycle of 60 s. The cooling coil is considered to be dry all the time; only the sensible heat is removed from the air (process 1–3 in Fig. 2). The process in the heating coil is represented in Fig. 2 by the transformation 2–3.

4.1. Dynamic model

The dynamic model of the heat exchanger may be obtained from the energy balance equation

$$m_C c_C \frac{d\theta_C}{dt} = P - \rho_a Q_a c_a(\theta_{a2} - \theta_{a1}), \tag{17}$$

where the left-hand term is the energy accumulation in the mass of the coil and the right-hand term is the difference between the energy rate delivered by the coil and that absorbed by the air. It will be assumed that the air temperature is changed by convective heat transfer:

$$\rho_a Q_a c_a(\theta_{a2} - \theta_{a1}) = U_C S_C\left(\theta_C - \frac{\theta_{a2} + \theta_{a1}}{2}\right). \tag{18}$$

In the case of the electric heater, the power P is delivered by the electric grid; in the case of the cooling coil, it is delivered by a water chiller. The temperature of the inlet air is considered as reference, which implies that

$$d\theta_{a1}/dt \equiv 0 \tag{19}$$

and

$$\Delta\theta_a \equiv \theta_{a2} - \theta_{a1}. \tag{20}$$

From (19) and (20) it results that

$$\frac{d\theta_{a2}}{dt} = \frac{d\,\Delta\theta_a}{dt}. \tag{21}$$

The transfer function of the heat exchanger is obtained by eliminating θ_c from (17) and (18) and by applying Laplace transform for zero initial conditions:

$$\frac{\Delta\theta_a}{P} = \frac{K_C}{1 + T_C s}, \tag{22}$$

where

$$K_C = (\rho_a Q_a c_a)^{-1} \tag{23}$$

and

$$T_C = m_C c_C\left(\frac{1}{2\rho_a Q_a c_a} + \frac{1}{U_C S_C}\right). \tag{24}$$

Note that for a constant air flow rate, the value of K_C is constant and the value of T_C is variable since the overall heat transfer coefficient depends on water velocity (ASHRAE, 2001c; McAdams, 1954):

$$U_C \propto v_w^{0.8}. \tag{25}$$

Corresponding respectively to the two terms of Eq. (24), the time constant of the cooling coil is formed of a constant term and a variable term which depends on the water flow rate which, in turn, is subject to the command of the three-way valve of the cooling coil:

$$T_C = T_{Ca} + \frac{T_{Cw}}{u^{0.8}}. \tag{26}$$

Eq. (26) is similar to the result obtained by Pearson et al. (1974) by expressing the coil model as a set of partial differential equations. The parameters K_C and T_C may be estimated from the design values of the coils by using Eqs. (23) and (24), or may be obtained by experimental identification.

The power P in Eq. (22) may be a linear or a nonlinear function of the command, u.

4.2. Actuator model for electric heaters

The actuator of the heating coil is a static relay which varies the electric power delivered to the coil from zero to 100% of the maximum power, P_M, according to the command, u:

$$P = uP_M. \tag{27}$$

Combining Eqs. (22) and (27), the transfer function of the system formed by the static relay and the electric coil becomes

$$\frac{\Delta\theta_a}{u} = \frac{K_C P_M}{1 + T_C s}. \tag{28}$$

Eq. (28) shows that the static gain, $K_C P_M$, is constant which implies that the static characteristic is linear with the slope $K_C P_M$ (Fig. 5a, lines HC_1 and HC_2). The dots in Fig. 5(a) correspond to the measured values from Table 1.

4.3. Actuator model for fluid-filled coils

The actuator of the cooling coil is a motor-driven three-way valve. The dynamic model of the positioner is of the first order with a time constant of 15 s, negligible in comparison with the other time constants. The three-way valve varies the power delivered to the coil. With the notations from Fig. 3, the steady-state energy balance equations applied to the cooling coil for maximum opening of the three-way valve are:

- the maximum power delivered by the coil:

$$P_M = Q_M \rho_w c_w(\theta_{w1M} - \theta_{w2M}), \tag{29}$$

- the maximum power received by the air:

$$P_M = \dot{m}_a c_a(\theta_{a2M} - \theta_{a1M}), \tag{30}$$

- the maximum power transferred from water to air:

$$P_M = US\left(\frac{\theta_{w2M} + \theta_{w1M}}{2} - \frac{\theta_{a2M} + \theta_{a1M}}{2}\right). \quad (31)$$

The energy balance equations in normal operation are

- the power delivered by water:

$$P = Q\rho_w c_w(\theta_{w1} - \theta_{w2}), \quad (32)$$

- the power received by the air:

$$P = \dot{m}_a c_a(\theta_{a2} - \theta_{a1}), \quad (33)$$

- the power transferred from water to air:

$$P = US\left(\frac{\theta_{w2} + \theta_{w1}}{2} - \frac{\theta_{a2} + \theta_{a1}}{2}\right). \quad (34)$$

Noting

$$p \equiv \frac{P}{P_M} \quad (35)$$

and

$$q \equiv \frac{Q}{Q_M}, \quad (36)$$

and dividing Eq. (32) by Eq. (29), it results in:

$$p = q\frac{\theta_{w1} - \theta_{w2}}{\theta_{w1M} - \theta_{w2M}}. \quad (37)$$

Dividing Eq. (33) by Eq. (30), it results in:

$$p = \frac{\theta_{a2} - \theta_{a1}}{\theta_{a2M} - \theta_{a1M}}. \quad (38)$$

Dividing Eq. (34) by Eq. (31), it results in:

$$p = \frac{(\theta_{w2} + \theta_{w1}) - (\theta_{a2} + \theta_{a1})}{(\theta_{w2M} + \theta_{w1M}) - (\theta_{a2M} + \theta_{a1M})}. \quad (39)$$

Introducing θ_{w2} from (37) and θ_{a2} from (38) into (39), it results in:

$$p = f(q, \theta_{w1}, \theta_{a1} \,|\, \theta_{w1M}, \theta_{w2M}, \theta_{a1M}, \theta_{a2M}). \quad (40)$$

Substituting θ_{w2} from (37) and θ_{a2} from (38) into (39), it results in:

$$p = 2(\theta_{a1} - \theta_{w1})\frac{q}{Aq + B} \quad (41)$$

with

$$A = 2\theta_{a1M} - \theta_{w2M} - \theta_{w1M} \quad (42)$$

and

$$B = \theta_{w2M} - \theta_{w1M}. \quad (43)$$

Eq. (41) shows that the static gain is nonlinear. From Eqs. (22), (35) and (41), it results that

$$\Delta\theta_a = K_C P_M p, \quad (44)$$

where K_c is given by Eq. (23), P_M is the maximum power available for the coil and p is given by Eq. (35). Considering relation (41), Eq. (44) becomes:

$$\Delta\theta_a = 2K_C P_M(\theta_{a1} - \theta_{w1})\left(\frac{q}{Aq + B}\right). \quad (45)$$

The flow rate in the cooling coil depends on the position of a three-way valve. If the three-way valve has a linear characteristic and if the hydraulic resistance of the balance valve is equal to that of the coil, then Eq. (45) allows us to represent the relation between the position of the three-way valve, q, and the air temperature difference of the cooling coil, $\Delta\theta_a$. Since relation (45) is linear in parameters, the parameters may be estimated from measurements by using linear regression. The curve CC in Fig. 5(a) shows the values of the static characteristic for a cooling coil. The dots are obtained experimentally (Table 1). The curves passing through the dots are obtained by regression from the experimental data and by using Eq. (45) for the design conditions of the studied cooling coil. The two curves are practically identical.

The nonlinear static characteristic of the cooling coil induces poor performance of the classical PI controller with constant parameters (Salsbury, 1999). The advantage of expressing the transfer function of the heat exchanger as variable static and dynamic gains is that the parameters of the controller can be easily scheduled according to the operating point of the coil.

4.4. Discrete model of the coils

Represented as a block diagram, the model of the coil is composed of a zero-order hold on the command, the actuator, the coil and the sensor (Fig. 4). The relation between the power and the command is linear for the electric coil, Eq. (27), and nonlinear for the fluid-filled coil, Eqs. (44) and (45). By considering the relation between power and command as linear for small variations around a static operating point, the transfer function of the system represented in Fig. 4 is

$$G_p(s) = \frac{1 - e^{-sT_S}}{s}\frac{K_C}{(1 + T_C s)(1 + T_T s)}e^{-s\tau}. \quad (46)$$

Note that for the water-filled coils, the local static gain, K_C, changes with the operating point according to Eq. (41) resulting in a nonlinear characteristic (Fig. 5).

The well-calibrated transducer has a unitary static gain; its time constant, T_T, is determined by using least mean square regression for the discrete model described in Section 3. Expanding transfer function (46) in partial fractions,

$$G_p(s) = \left(1 - e^{-sT_s}\right) \times e^{-s\tau}K_C\left[\frac{1}{s} + \frac{T_C^2/(T_T - T_C)}{1 + T_C s} + \frac{T_T^2/(T_C - T_T)}{1 + T_T s}\right] \quad (47)$$

and putting Eq. (47) in the form of state-space model gives:

$$\dot{\mathbf{x}} = \mathbf{A}\mathbf{x} + \mathbf{B}\mathbf{u},$$
$$\mathbf{y} = \mathbf{C}\mathbf{x} + \mathbf{D}\mathbf{u}, \tag{48}$$

where

$$\mathbf{A} = \begin{bmatrix} -\frac{T_C+T_T}{T_C T_T} & -\frac{1}{T_C T_T} \\ 1 & 0 \end{bmatrix}, \quad \mathbf{B} = \begin{bmatrix} \frac{K_C}{T_C T_T} \\ 0 \end{bmatrix},$$

$$\mathbf{C} = \begin{bmatrix} 0 & 1 \end{bmatrix}, \quad \mathbf{D} = 0.$$

The discrete transfer function is obtained by using the z transform of each term of Eq. (47):

$$G_p(z) = K_C z^{-k} \frac{z-1}{z}\left(\frac{z}{z-1} + \frac{T_C}{T_T - T_C}\frac{z}{z - \mathrm{e}^{-T_s/T_C}} + \frac{T_T}{T_C - T_T}\frac{z}{z - \mathrm{e}^{-T_s/T_T}}\right) \tag{49}$$

or

$$G_p(z) = \frac{\beta_1 z + \beta_0}{z^2 + \alpha_1 z + \alpha_0}, \tag{50}$$

where

$$\beta_1 = K_C \frac{T_C \mathrm{e}^{-T_s/T_C} - T_T \mathrm{e}^{-T_s/T_T} - T_C + T_T}{T_T - T_C},$$
$$\beta_0 = K_C \frac{(T_T - T_C)\mathrm{e}^{-T_s/T_c}\mathrm{e}^{-T_s/T_T} + T_C \mathrm{e}^{-T_s/T_T} - T_T \mathrm{e}^{-T_s/T_c}}{T_T - T_C}$$
$$\alpha_1 = -\left(\mathrm{e}^{-T_s/T_c} + \mathrm{e}^{-T_s/T_T}\right), \quad \alpha_0 = \mathrm{e}^{-T_s/T_c}\mathrm{e}^{-T_s/T_T}.$$

Writing Eq. (50) in the state-space form gives the discrete model of the coils:

$$z\mathbf{x} = \mathbf{F}\mathbf{x} + \mathbf{G}\mathbf{u},$$
$$\mathbf{y} = \mathbf{H}\mathbf{x} + \mathbf{D}\mathbf{u}, \tag{51}$$

where

$$\mathbf{F} = \begin{bmatrix} -\alpha_1 & -\alpha_0 \\ 1 & 0 \end{bmatrix}, \quad \mathbf{G} = \begin{bmatrix} \beta_1 \\ 0 \end{bmatrix}, \quad \mathbf{H} = \begin{bmatrix} 1 & \frac{\beta_0}{\beta_1} \end{bmatrix}, \quad \mathbf{D} = 0. \tag{52}$$

4.5. Identification of the grey-box model parameters

The parameters of the model given by Eq. (50) may be identified by following the procedure described in Section 3. However, this procedure does not take advantage of the existing knowledge about the system; it does not use the parameters identified for the sensor.

The models (48) and (51), the equivalent state-space form of model (50), have coupled parameters. The parameters of the coil, K_C and T_C, are unknown and the time constant of the sensor, T_T, is known (being identified by using the model and the procedure described in Section 3). The idgrey model in continuous time may be used to solve this identification problem (Ljung, 2005). The model is of the form given by

$$\dot{\mathbf{x}} = \mathbf{A}\mathbf{x} + \mathbf{B}\mathbf{u} + \mathbf{K}\mathbf{w},$$
$$\mathbf{y} = \mathbf{C}\mathbf{x} + \mathbf{D}\mathbf{u} + \mathbf{w}, \tag{53}$$

where

$$\mathbf{A} = \begin{bmatrix} -\frac{T_C+T_T}{T_C T_T} & -\frac{1}{T_C T_T} \\ 1 & 0 \end{bmatrix}, \quad \mathbf{B} = \begin{bmatrix} K/(T_C T_T) \\ 0 \end{bmatrix}$$

$$\mathbf{C} = \begin{bmatrix} 0 & 1 \end{bmatrix}, \quad \mathbf{D} = 0, \quad \mathbf{K} = \begin{bmatrix} 0 \\ 0 \end{bmatrix}$$

and the initial condition $\mathbf{x}_0 = \begin{bmatrix} 0 & 0 \end{bmatrix}^{\mathrm{T}}$. The additive noise, $\mathbf{w}$, in model (53) is negligible and the Kalman gain, $\mathbf{K}$, is put to zero. The matrices $\mathbf{A}$, $\mathbf{B}$, have partly known elements. The predictor of (53) takes the form:

$$\hat{\mathbf{x}}(t + T_s) = \mathbf{F}(\boldsymbol{\psi})\mathbf{x}(t) + \mathbf{G}(\boldsymbol{\psi})\mathbf{u}(t) + \mathbf{K}(\boldsymbol{\psi})(\mathbf{y}(t) - \mathbf{C}(\boldsymbol{\psi})\hat{\mathbf{x}}(t)),$$
$$\hat{\mathbf{y}}(t\boldsymbol{\psi}) = \mathbf{C}(\boldsymbol{\psi})\hat{\mathbf{x}}(t), \tag{54}$$

where $\mathbf{F}$ and $\mathbf{G}$ are computed from $\mathbf{A}$, $\mathbf{B}$, $\mathbf{C}$ and the sampling interval T_s according to Eq. (52). Note that if the model has m inputs, p outputs and n states, a maximum of $(p+m)n$ parameters associated with $\mathbf{A}$, $\mathbf{B}$, $\mathbf{C}$ can be estimated (Parrilo & Ljung, 2003). It will be considered the *output error case* when w is zero, which implies that $\mathbf{K} = 0$. The unknown parameters $\boldsymbol{\psi}$ are estimated by minimizing the prediction error:

$$V_N(\boldsymbol{\psi}) = \sum_{t=1}^{N} \left[y(t) - \hat{y}(t|\boldsymbol{\psi})\right]^2 \tag{55}$$

with respect to $\boldsymbol{\psi}$. The global minimum of (55), denoted by $\hat{\boldsymbol{\psi}}_N$, is found by iterative search by using a damped Gauss–Newton method (Ljung, 1999, 2005):

$$\hat{\boldsymbol{\psi}}_N^{(i+1)} = \hat{\boldsymbol{\psi}}_N^{(i)} + \mu \mathbf{R}_N^{(i)} V_N^{\mathrm{T}}(\hat{\boldsymbol{\psi}}_N^{(i)}), \tag{56}$$

where $\mathbf{R}_N^{(i)}$ is the gain matrix and μ is a weighting factor used to normalize the gain (Ljung, 1999).

The search method (56) requires an initial value of the parameter value, $\hat{\boldsymbol{\psi}}_N^{(0)}$. Depending on the value of the initial guess, the iterations $\hat{\boldsymbol{\psi}}_N^{(i)}$ may not converge, converge to a local minimum or converge to the desired value of the global minimum. Thus, the initial value of the parameter estimates should lie in the domain of attraction of the global minimum (Parrilo & Ljung, 2003; Wernholt, 2004).

5. Parameter identification of the humidifier model

In other studies, the humidifier was modelled as a first-order transfer function with the time constant coming from the "capacity" of the humidifier (Kramer, 2003; Tashtoush et al., 2005). Since the steam is directly injected into the air stream, the humidifier increases instantaneously the humidity ratio (or the moisture content) of the inlet air. The process is described by the mass and the energy balance equations (ASHRAE, 2001a):

$$\dot{m}_{da}W_1 + \dot{m}_w = \dot{m}_{da}W_2,$$
$$\dot{m}_{da}h_1 + \dot{m}_w h_w = \dot{m}_{da}h_2. \tag{57}$$

From the mass balance equation, it results that the increase in the moisture content is the ratio between the mass flows of the steam and of the dry air:

$$\Delta W \equiv W_2 - W_1 = \frac{\dot{m}_w}{\dot{m}_{da}}. \tag{58}$$

In steam humidifiers, the steam is injected directly into the air stream. Since the mixing phenomenon is practically instantaneous, the transfer function of the humidifier is characterized only by the transport time of the steam from the steam generator to the stem located inside the air current:

$$\frac{\Delta W}{u} = \frac{\dot{m}_{wM}}{\dot{m}_{da}} \mathrm{e}^{-\tau s}, \tag{59}$$

where u is the command of the humidifier. The identification of this model consists simply in measuring the static gain, $\dot{m}_{wM}/\dot{m}_{da}$, and the transport time, τ. The static characteristic of the steam humidifier is shown in Fig. 5(b). The dots represent the measured values, which correspond to those from Table 1, and the line represents the linear regression obtained by using the measurements. The fact that the characteristic does not pass through the origin is due to the time-proportional command and the transport time from the steam generator to the stem inside the AHU; when the command is smaller than 20%, the time for which the command is "on" is shorter than the transport time.

6. Secondary outputs

The modelling approach presented in this paper assumes constant airflow in the AHU. The elements of the AHU cause the variation of the primary variables: dry-bulb temperature for the coils and humidity ratio for the steam humidifier. The second output of each element, i.e. humidity for the coils and temperature for the humidifier, are a result of the variation of the primary output.

When the controlled variables are temperature and relative humidity, the secondary variables may be calculated using the relations for the humid air (ASHRAE, 2001b). Note that the humidification by direct steam injection is almost an isothermal process because the temperature of the air remains almost constant as the moisture is added; the temperature increases typically with 1 °C (ASHRAE, 2001b). Knowing the inlet temperature, the temperature increase may be calculated from the system of Eqs. (57).

7. Experimental protocol and results discussion

The experimental procedure consists in two stages. First, the transfer function of the sensor is identified. The sensor is extracted from the AHU, left outside the AHU for about 5 min and then reinserted in the AHU. The step response is logged and the model is identified by using the procedure described in Section 3. Second, a step command of 20–25% of the total range is given to an element (e.g. heating coil, cooling coil or humidifier). Then, the difference between the outlet and the inlet value is calculated. The parameters of the grey model are identified as described in Section 4.

Fig. 6 shows the command and the temperatures of a heating coil and the comparison between the measured output and the model. Note that the output of the coil is the temperature difference between the outlet and the inlet air, $\Delta\theta$. The difference eliminates the trend in the output that is caused by the variability in the inlet value. The small variations of the outlet temperature, θ_{out}, are due to the time-proportional command. The inlet temperature, θ_{in}, has also a ripple due to the turbulence and recirculation of the air in the AHU. The cycle rate selected was of 1 min; consequently, in Fig. 6(b) the output, $\Delta\theta$, has an oscillation period of 1 min.

Fig. 7 shows the results for the cooling coil for a step command from 25% to 50%. The temperatures have a variation cycle of about 15 min due to the variation of the water temperature provided by the chiller. The temperature control of the cold water delivered by the chiller is on–off with the limit values 7–10 °C. The variation of the cold water will be reflected in the variation of the outlet air temperature, θ_{out}. Note in Fig. 7(a) that the inlet air temperature, θ_{in}, varies too; this phenomenon is due to the turbulent airflow upstream the cooling coil: the air flow hits

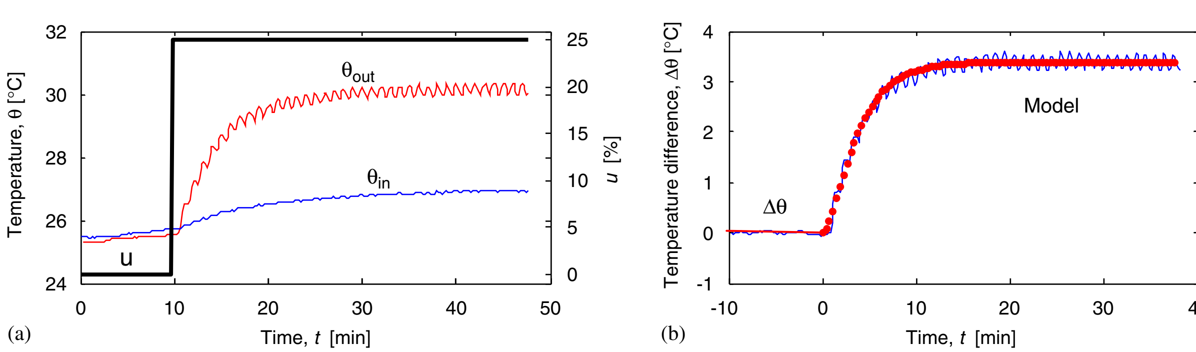

Fig. 6. Identification of the dynamic model of the electric coil 1: (a) experimental data; (b) comparison between the measured temperature difference and the grey-box model.

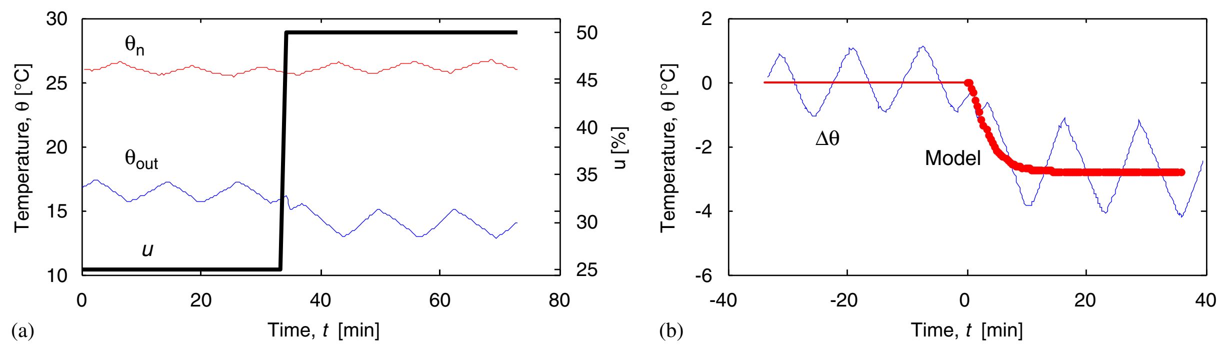

Fig. 7. Identification of the dynamic model of the cooling coil: (a) experimental data; (b) comparison between the measured temperature difference and the grey-box model.

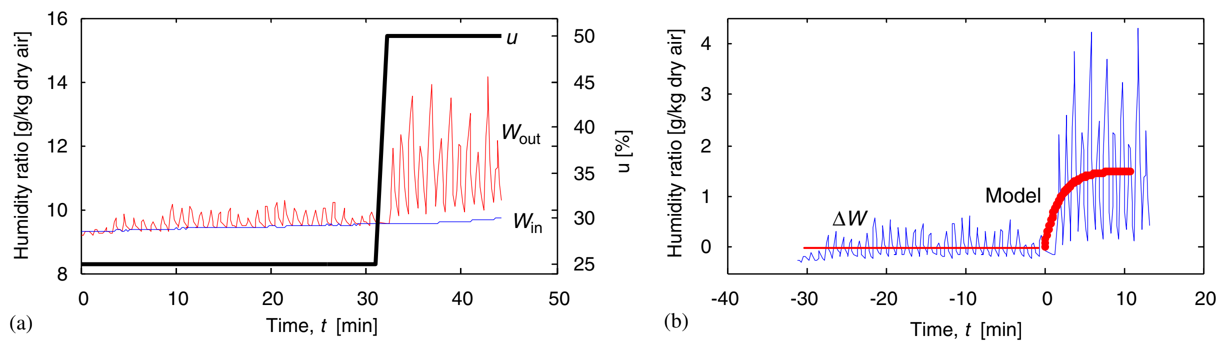

Fig. 8. Identification of the dynamic model of the humidifier: (a) experimental data; (b) comparison between the measured humidity ratio difference and the grey-box model.

the coil and then is returned back to the sensor. In Fig. 7(b) note that the start and the end points of the sequence of the temperature difference, $\Delta\theta$, were chosen to not influence the mean on the sequence before and after the change in the command.

Fig. 8 shows the results for the humidifier. The command of the humidifier is time-proportional; the cycle rate used was 1 min. The transfer function of the humidifier is a pure time delay (see Section 5). If the command is shorter than about 10 s, then the humidifier injects no steam in the AHU. Fig. 5(b) shows that the static characteristic is zero if the command is less than 18%, which corresponds to about 10 s for a cycle rate of 1 min. For the case shown in Fig. 8, the command was varied from 25%, when the humidifier injected 4 g/kg for 15 s minus 10 s (the transport time), i.e. for 5 s during a minute, to 50%, when it injected 4 g/kg for 30 s minus 10 s (the transport time), i.e. for 20 s per minute. The on–off commands of the humidifier are reflected in the variations of the humidity ratio of the outlet air, W_{out}. The measured values of the humidity ratio, W_{out}, are filtered by the humidity sensor.

The causes of the high noise–signal ratio of the cooling coil (Fig. 7b) and of the humidifier (Fig. 8b) are of different nature. In the first case, it is the maximum power that the coil can deliver that varies; due to its low frequency compared with the frequency pass band of the coil, this disturbance will be rejected by the control system. In the second case, the time-proportional on/off command of the humidifier and its lack of inertia generate the noise; this noise cannot be reduced by the control system. However, the value of the humidity is averaged in the air-distribution system and in the conditioned space.

The grey-box model, which takes into account the time constant of the sensor, gives the mean output of the AHU elements (Figs. 6b, 7b and 8b). This approach improves the parameter identification of discrete low-order models which otherwise will bias to fit the noise. Table 3 gives a comparison of three methods of parameter identification: two black-box models derived from continuous models, one with one time constant and the other with two time constants, and a grey-box model in which the model of the sensor is known. All methods identified correctly the static gain, K_C. The first-order discrete model is, in fact, a reduced model of the second-order model. The identified time constants for the second-order discrete model (obtained from the second-order continuous model) do not represent the real values: time constant T_1 is very little showing that the model biased to fit the noise. In the grey-box model, accounting for the sensor model results in a correct identification of the time constant of the coil, T_C. The two time constants, that of the coil and that of the sensor, may be used in tuning the controller.

8. Model validation

The basic validation technique is to compare the simulation results with the measurements. In addition,

Table 3
Identified parameters of the heating coil HC_1

Command step (%)	Discrete model					Grey model	
	With one time constant		With two time constants				
	K_C	T	K_C	T_1	T_2	K_C	T_C
0–25	13.60	3.42	13.03	0.19	2.72	13.54	2.91
25–50	13.80	3.26	13.65	0.23	1.91	13.57	3.30
50–75	12.40	2.31	12.04	0.10	2.34	12.36	2.62
75–100	11.30	2.56	11.70	0.05	4.11	11.75	2.80

The parameters of the temperature sensor identified by using the discrete model are $K_T = 1.03$ and $T_T = 1.1$.

the identification approach presented in Sections 3 and 4 allows multiple crosschecking. The results obtained by using the identification of the model parameters from step response may be easily compared with the results of classical graphical methods. The dynamic model of the transducer has two parameters: K_T and T_T which may be calculated from the three parameters of the model: a_1, b_0 and b_1, and from the static gain expressed by Eq. (16). If the parameters K_T and T_T calculated from these values are nearly equal, the identification is correct. Similarly, the parameters of the coils, K_C and T_C may be calculated from the three elements of the state-space model described by Eq. (53) and from the expression of the static gain similar to Eq. (16); again, if the values obtained by using these informations are nearly equal, the identification is correct.

The comparison of the values of the static gain obtained by using Eqs. (6) and (16) shows if the identification is correct. The values of the static gain may be compared with the theoretical estimations obtained from the steady-state models: Eq. (27) for the electric coil, and Eq. (41) for the fluid-filled coil. Fig. 5(a) shows the comparison between the static gains obtained by identifying the parameters of the grey-box model (48) with the procedure (56) and by modelling using Eq. (27) for the electric coil and Eq. (45) for the fluid-filled coil. The comparison shows practically no difference between the model and the measured data. Fig. 5(b) shows the static characteristic of the humidifier. The static gain is linear, as predicted by the theory. The fact that the static characteristic does not begin in zero is due to the time-proportional command of the humidifier: while the command is shorter than the transport time, the steam is not injected.

9. Conclusions

The AHU with constant air volume is a MIMO system. The inputs are the commands of the AHU elements: the cooling coil, the heating coil and the humidifier. The outputs are the dry-bulb air temperature and humidity ratio (i.e. moisture content) of the supply air.

If the outputs of the AHU elements are considered to be the temperature difference for the coils and the humidity ratio difference for the humidifier, and if the cooling coil is dry (i.e. no dehumidification by cooling), then the individual processes in the AHU are decoupled. This allows us to define separate transfer functions for each element. Each element changes a single output which is considered in the transfer function, i.e. temperature for the coils and humidity ratio for the humidifier. When the controlled variables are temperature and relative humidity, the other output, i.e. relative humidity for the coils and temperature for the humidifier, is calculated from the primary output of the transfer function by using the relations for the humid air.

The transfer function of the coils relates the temperature difference between the outlet and the inlet air to the command. This paper demonstrates that, in the case of sensible heat exchange (no dehumidification by cooling), the transfer function may be written as a product of a static and a dynamic gain. These gains are constant for the electric coils and variable for the fluid-filled coils. The advantage of writing the transfer function as a product of a static and a dynamic gain is that the model can be easily linearized by scheduling the gains in function of the operation point. The steam humidifier is characterized by a linear static gain.

The theoretical analysis gives the form of the models. The experimental identification of the parameters is done for the discrete form of the models obtained by applying the bilinear transform. Step inputs were used for the sensors and for the AHU elements. It was found that in industrial applications, the dynamic gain of the transducers is almost equal to that of the elements. Therefore, the identification of the elements takes into account the model of the sensor, model that has been identified separately. The procedure for finding the parameters of the AHU elements uses an iterative optimization of the estimation in order to minimize the prediction error of a grey-box model.

The grey-box identification proposed in this paper uses the theoretical knowledge and the known parameters of the sensors identified in separate experiments. The result consists in dynamic models ready to be used in simulation software and in control algorithm synthesis. The practical advantage of having separate time constants for the sensors and the AHU elements is that the PID tuning may be done directly by using these values. Thus, the time consumed for identification pays off by reducing the time needed for manual tuning. Once the controller is tuned, its parameters do not need to be changed because the model of the process, as it was formulated in this paper, may be linearized. The linearization may be considered equivalent to gain scheduling but the advantage of expressing the models in a linear form is that the controller parameters do not need to be changed on the whole range of operation. The cost of this solution is the supplementary temperature and humidity transducer which measures the properties of the mixed air.

References

ASHRAE. (1999). Supervisory control strategies and optimization. In: *ASHRAE handbook HVAC applications* (pp. 40.1–40.36). American Society of Heating, Refrigerating, and Air Conditioning Engineers, Inc.

ASHRAE. (2001a). Humidifiers. In: *ASHRAE handbook of fundamentals 2001* (pp. 20.1–2.10). American Society of Heating, Refrigerating, and Air Conditioning Engineers, Inc.

ASHRAE. (2001b). Psychrometrics. In: *ASHRAE handbook of fundamentals 2001* (pp. 6.1–6.17). American Society of Heating, Refrigerating, and Air Conditioning Engineers, Inc.

ASHRAE. (2001c). Heat transfer. In: *ASHRAE handbook of fundamentals 2001* (pp. 3.1–3.27). American Society of Heating, Refrigerating, and Air Conditioning Engineers, Inc.

Bi, Q., Cai, W.-J., Wang, Q.-G., Hang, C.-C., Lee, E.-L., Sun, Y., et al. (2000). Advanced controller auto-tuning and its application in HVAC systems. *Control Engineering Practice*, *8*(6), 633–644.

Clarke, J. A., Cockroft, J., Conner, S., Hand, J. W., Kelly, N. J., Moore, R., et al. (2002). Simulation-assisted control in building energy management systems. *Energy and Buildings*, *34*(9), 933–940.

COSTIC. (2003). *Réglementation de l'Equipement Technique du Bâtiment V01-03*. St. Remy les Chevreuse.

Deng, S. (2002). The application of feedforward control in a direct expansion (DX) air conditioning plant. *Building and Environment*, *37*(1), 35–40.

Gartner, J. R. (1972). Simplified dynamic response relations for finned-coil heat exchangers. *ASHRAE Transactions*, *78*(2), 163–168.

Gartner, J. R., & Daane, L. E. (1969). Dynamic response relations for a serpentine crossflow heat exchanger with water velocity disturbance. *ASHRAE Transactions*, *75*(1), 53–67.

Gartner, J. R., & Harrison, H. L. (1963). Frequency response transfer functions for a tube in crossflow. *ASHRAE Transactions*, *69*, 323–330.

Gartner, J. R., & Harrison, H. L. (1965). Dynamic characteristics of water-to-air crossflow heat exchangers. *ASHRAE Transactions*, *71*, 212–224.

Ghiaus, C. (1996). *Intelligent control of HVAC systems*. PhD thesis, Technical University of Civil Engineering of Bucharest, Romania.

Ghiaus, C. (2001). Fuzzy model and control of a fan-coil. *Energy and Buildings*, *33*(6), 545–551.

Howell, J. (1988). Relative humidity in HVAC systems: Improving control. *Building Services Engineering Research and Technology*, *9*(2), 55–61.

Jin, G.-Y., Cai, W.-J., Wang, Y.-W., & Yao, Y. (2005). A simple dynamic model of cooling coil unit. *Energy Conversion and Management*, *47*(15–16), 2659–2672.

Jonsson, G., & Palsson, O. P. (1994). An application of extended Kalman filtering to heat exchanger models. *Journal of Dynamic Systems, Measurement, and Control*, *116*, 257–264.

Kramer, R. (2003). *System integration of distributed power for complete building systems*. Golden, CO: National Renewable Energy Laboratory p. 258.

Levermore, G. (2000). *Building control systems—CIBSE guide H*. Oxford, UK: Butterworth-Heinemann.

Ljung, L. (1999). *System identification—Theory for the user*. Upper Saddle River, NJ: Pretince Hall PTR.

Ljung, L. (2005). *System identification toolbox*. Natick, MA: The MathWorks Inc.

Mathews, E. H., & Botha, C. P. (2003). Improved thermal building management with the aid of integrated dynamic HVAC simulation. *Building and Environment*, *38*(12), 1423–1429.

McAdams, W. H. (1954). *Heat transmission*. New York: McGraw-Hill.

Pakanen, J. E., & Sundquist, T. (2003). Automation-assisted fault detection of an air-handling unit; implementing the method in a real building. *Energy and Buildings*, *35*(2), 193–202.

Parrilo, P., & Ljung, L. (2003). *Initialization of physical parameter estimates*. Linkoping, Sweden: Linkoping Universitet p. 9.

Pearson, J. T., Leonard, R. G., & McCutchan, R. D. (1974). Gain and time constant for finned serpentine crossflow heat exchangers. *ASHRAE Transactions*, *80*(2), 255–267.

Salsbury, T. I. (1999). A practical algorithm for diagnosing control loop problems. *Energy and Buildings*, *34*(4), 429–449.

Salsbury, T. I. (2002). A new pulse modulation adaptive controller (PMAC). *Control Engineering Practice*, *10*(12), 1357–1370.

Salsbury, T. I. (2006). Continuous-time identification for closed loop control performance assessment. *Control Engineering Practice*, *15*(1), 109–121.

Shin, Y., Chang, Y. S., & Kim, Y. (2002). Controller design for a real-time air handling unit. *Control Engineering Practice*, *10*(5), 511–518.

Singh, G., Zaheer-uddin, M., & Patel, R. V. (2000). Adaptive control of multivariable thermal processes in HVAC systems. *Energy Conversion and Management*, *41*(15), 1671–1685.

So, A. T. P., Chan, W. L., Chow, T. T., & Tse, W. L. (1995). New HVAC control by system identification. *Building and Environment*, *30*(3), 349–357.

Sousa, J. M., Babuska, R., & Verbruggen, H. B. (1997). Fuzzy predictive control applied to an air-conditioning system. *Control Engineering Practice*, *5*(10), 1395–1406.

Tashtoush, B., Molhim, M., & Al-Rousan, M. (2005). Dynamic model of an HVAC system for control analysis. *Energy*, *30*(10), 1729–1745.

Thompson, R., & Dexter, A. (2005). A fuzzy decision-making approach to temperature control in air-conditioning systems. *Control Engineering Practice*, *13*(6), 689–698.

Tobi, T., & Hanafusa, T. (1991). A practical application of fuzzy control for an air-conditioning system. *International Journal of Approximate Reasoning*, *5*(3), 331–348.

Underwood, C. P. (1999). *HVAC control systems: Modeling, analysis and design*. London and New York: E & FN Spon.

Wang, S., & Jin, X. (2000). Model-based optimal control of VAV air-conditioning system using genetic algorithm. *Building and Environment*, *35*(6), 471–487.

Wang, S., & Xu, X. (2002). A robust control strategy for combining DCV control with economizer control. *Energy Conversion and Management*, *43*(18), 2569–2588.

Wang, S., & Zheng, L. (2001). Dynamic and real-time simulation of BMS and air-conditioning system as a 'living' environment for learning/training. *Automation in Construction*, *10*(4), 487–505.

Wang, Y.-W., Cai, W.-J., Soh, Y.-C., Li, S.-J., Lu, L., & Xie, L. (2004). A simplified modeling of cooling coils for control and optimization of HVAC systems. *Energy Conversion and Management*, *45*(18–19), 2915–2930.

Wernholt, E. (2004). *On multivariable and nonlinear identification of Industrial robots* (p. 139). Linkoping, Sweden: Division of Automatic Control and Communication Systems, Linkoping University.